JOURNAL OF SUSTAINABLE MINING

Volume 23 | Issue 2 Article 6

2024

Difficulties of hydrofracturing in sandstone – experimental study

Author(s) ORCID Identifier:
S. Vikram: 0000-0001-7145-7487
Dheeraj Kumar: 0000-0002-0321-056X
DS Subrahmanyam: 0000-0003-4549-5193

Recommended Citation

Vikram, S; Kumar, Dheeraj; and Subrahmanyam, DS (2024) "Difficulties of hydrofracturing in sandstone – experimental study," *Journal of Sustainable Mining*: Vol. 23 : Iss. 2 , Article 6.
Available at: https://doi.org/10.46873/2300-3960.1413

Difficulties of hydrofracturing in sandstone – experimental study

Abstract

Hydrofracturing in sandstone is not an easy task. Sandstone is porous; fluid dissipation is common hence unable to obtain breakdown pressures in certain flow rates (0.0000005–0.0001 m3/s). The higher flow rate (0.00025 m3/s) is ascertained to determine the fracturing pressures. Due to this, fracture propagation and delineation are observed [1]. To enhance, an experimental method is adopted by carrying out 6 Hydrofracturing tests in a borehole comprising sandstone. A high flow rate of 0.00025 m3/s and viscosity 0.001 Pascal second is applied. Later, the fracture simulation was run on 12 core samples collected from the same depths in a lab. The fluid flow rates of 0.0000005–0.0000015 m3/s, viscosity 0.27 Pascal-second, pore pressure of 4 MPa, confining pressures in vertical-12 MPa and horizontal 6, 18, 24, 30 MPa is applied. The fracture traces and the stress results exhibit a difference of 80 to 300 observed in both cases. The major principle stress orientation obtained in the borehole is 20 and 40. In lab tests with confining horizontal pressures at 6 and 18 MPa, it is 120 and 130, and at 24 and 30 MPa is 20. This indicated that there is fracture delineation occurred. It is observed in the higher flow rate and confining pressures.

Keywords

High flow rate; Hydraulic fracturing; Shut-in pressure; Anisotropy; Coal reserves; fractured and porous rock mass

RESEARCH ARTICLE

Difficulties of hydrofracturing in sandstone – Experimental study

S. Vikram [a,*], Dheeraj Kumar [b], D. S. Subrahmanyam [c]

[a] Research Scholar, IIT (ISM) Dhanbad, India
[b] Professor, IIT (ISM) Dhanbad, India
[c] Scientist, NIRM, India

Abstract

Hydrofracturing in sandstone is not an easy task. Sandstone is porous; fluid dissipation is common hence unable to obtain breakdown pressures in certain flow rates (0.0000005–0.0001 m^3/s). The higher flow rate (0.00025 m^3/s) is ascertained to determine the fracturing pressures. Due to this, fracture propagation and delineation are observed (Satya Subrahmanyam, 2022) [1].

To enhance, an experimental method is adopted by carrying out 6 Hydrofracturing tests in a borehole comprising sandstone. A high flow rate of 0.00025 m^3/s and viscosity 0.001 Pa s is applied. Later, the fracture simulation was run on 12 core samples collected from the same depths in a lab. The fluid flow rates of 0.0000005–0.0000015 m^3/s, viscosity 0.27 Pa-second, pore pressure of 4 MPa, confining pressures in vertical-12 MPa and horizontal 6, 18, 24, 30 MPa is applied.

The fracture traces and the stress results exhibit a difference of 80°–300° observed in both cases. The major principle stress orientation obtained in the borehole is 20° and 40°. In lab tests with confining horizontal pressures at 6 and 18 MPa, it is 120° and 130°, and at 24 and 30 MPa is 20°. This indicated that there is fracture delineation occurred. It is observed in the higher flow rate and confining pressures.

Keywords: high flow rate, hydrofracturing, shut-in pressure, anisotropy, coal reserves, fractured and porous rock mass

1. Introduction

Sedimentary strata generally occur in marine or lacustrine environments and form a series of layers. The strata remain horizontal and not too contorted or faulted. Hydrofracturing in sandstone generates rubble, which makes it difficult to obtain shut-in pressures [1]. The required shut-in pressures could not be able to build up, and there was a sudden drop in fracturing pressures [2]. Several studies have been carried out to understand the behaviour and provide alternate solutions, especially in the case of sandstone [3,4].

Determining stresses in sandstone varies significantly. It is due to rock stiffness. Stress may increase or decrease due to its unability to build up potential. Hence, it is best to understand stress re-distribution around. The grain structure, spacing between granules, porosity index, joint thickness and extent of discontinuities may alter the stress regime. These parameters may differ and act as anomaly [5]. Calculation of stress in sandstone is useful. Without proper information on the source of arriving fracture breakdown, opening and closing, it is highly difficult to understand the hydrofrac process [6].

Hydrofracturing in mudstones, shales and sandstones is performed through perforations for benefict in the extraction of crude oil [7]. Here, the minor principle stress viz normal stress across the fracture is measured as breakdown pressure and instantaneous shut-in pressure. Instantaneous shut-in pressure is measured using small flow ranges 0.0000005 m^3/s to 0.000001 m^3/s, which gives reproductive results [8]. But the unusual behaviour in instantaneous shut-in pressures has always raised concern. Obtaining instantaneous shut-in pressures here is still unclear, and the problem appears to be complex in different lithologies [9].

Minor principle stress plays a vital role in oil and natural gas exploration [10]. The principle of

Received 8 May 2023; revised 3 November 2023; accepted 6 November 2023.
Available online 25 February 2024

* Corresponding author.
E-mail address: vikram.shankar.2015dr1097@me.iitism.ac.in (S. Vikram).

https://doi.org/10.46873/2300-3960.1413

hydrofracturing says that the shut-in pressure measured across the fracture is equivalent to minor principle stress. There is a difference between the instantaneous shut-in and the fracture closing pressures. As discussed, the low flow rates are favourable for measuring minor in-situ stress [11]. The low injection rate is used to measure the instantaneous shut-in and closing pressures [12]. At some instants, both pressures will be equal because the liquid viscosity is low and the injection rate is less [13].

Open-hole stress measurements are preferable for determining the major principle stress [14]. However, it is impractical in sandstone [15]. Whilst performing fracturing in casing and perforation in the borehole causes additional problems due to random perforation and annulus [16]. But sometimes, hydrofracturing through carefully designed perforations yields the same results as open. The purpose of the perforations is to create a provision for smooth and undisturbed passage of liquid in the rock with less damage [17]. Lengthy propagation in fractures is not necessary and can be detrimental if the perforations are close enough and compact [18,19]. Small perforations are suitable for soft or high-porous rock. To perform through perforations, several factors like fluid flow rate, volume and interpretation procedure play a major role [20].

During hydrofracturing in sandstones, the minimum downhole injection pressure required to hold open and extend a fracture is slightly more than the stress normal to the plane of the fracture. In this case, there will be a tendency for a fracture to delineate [21]. In general, during fracturing process, the pressure leads to swelling and shrinking with change in pore pressures. The increase in fluid flow of more than 0.000001 m^3/s than normal

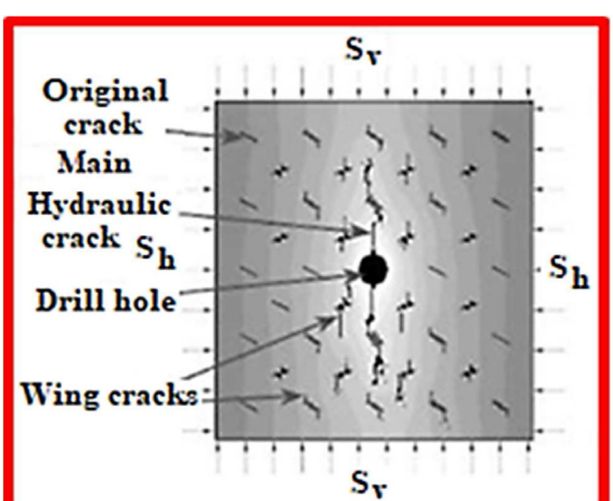

Fig. 1. Induced fracture/reopening of existing cleats by high flow rate.

(0.0000005 m^3/s) could change pore pressure but couldn't be able to measure the fracture closing pressure [22] (Fig. 1). This occurs due to the dissipation of the required pressure when the pore pressure is high.

The main barrier for fluid loss and slippage is the presence of pore pressures. The problem for leak-off is loss of fluid. This anomaly is most common in sandstone [23]. In sandstone, due to the core drilled borehole, the fines may be generated, which can cause the strata to be friable. These fines sometimes block the perforations [24]. Higher pressures are necessary in such case to obtain fracture closure with normal pressure from 0.02 to 0.027 MPa/m in a well bore. The pressure required to initiate the fracture may be 0.68 MPa or greater [25]. However, as discussed earlier, multiple pores may get opened, and there may be fracture deviation [26].

The fluid with a low flow rate of 0.000001 m^3/s or less would scatter in the perforations [27]. Consequently, pressurization leads to different orientations [28]. Thus, a new interpretation technique is required. Normal flow rate (0.0000005 m^3/s to 0.000001 m^3/s) is suitable for elastic medium and gives better results [29], while in non-elastic media like porous rocks, breakdown pressures get null and void. No data will be available for determining in-situ stress components [30]. Generally, in an elastic medium, pore pressures form a hydrostatic head. The intact rock having low permeability and a void ratio less than 0.03 shows little effect on pore pressures, which is negligible [31].

Repeated pressurization in elastic media ensures that the major influence of wellbore and rock tensile strength are overcome [32]. The effects of non-elasticity on medium dissolute the breakdown, closing and reopening pressures [33]. The injection rates must be sufficiently high to cross the natural permeability of the rock mass. An injection rate of too low may become partially permeable, resulting in additional pore pressures; in turn, pore pressures may alter [34].

Fracture closing pressure can only be a measure of the stress in hydrofracturing that is required to determine the results [35]. In flow rates of 0.000001–0.0000015 m^3/s with a viscosity of more than 0.39 Pa-second, the injection pressure will take more time to arrive at nil position, and it's not indicative of a stress level. In flow rates of 0.0000005 m^3/s to 0.000001 m^3/s with viscosity of 0.085–0.14 Pa-second, fracture closes rapidly, where the point to determine fracture closing pressure is not sufficient [36]. This pressure is small for sufficient large fracture. However, in some cases, with a small flow rate, fractures may be narrow, which induces a large pressure drop [37].

The dissipation of additional liquids in leftover joints is in between the rock structures. This opening is closer, and the span is wider enough such that a lesser flow rate can be dissipated [38]. This variation in flow rate needs to be modelled to obtain accurate fracture closing pressure [39]. If the fluid leak-off coefficient is reduced, the fracture closing pressure occurs very much low [40].

In low permeable rock formations, the fracture closing pressure does not drop fast because of lesser chances in fracture extension. The fracture extension requires large pressures [41]. Cornet has developed an analysis for determining the fracture closing pressures that consider a gradual increment in stress with respect to rock cover as an assumption. This cannot be validated in all aspects because of the presence of discontinuities such as faults and joints. This influences the stress regime [42].

Despite extensive studies, only limited investigations were performed in sandstone. Haimson, in his study, observed that, due to an increase in pore pressures, arbitrary stress conditions are developed, which in turn generate false implications [43]. This paper brings detailed discussions on the experimental studies carried out and their outcomes. How does it help carry out hydrofracturing in sandstones and mitigate obtaining breakdown pressures?

2. Structural changes in the sandstone induced by hydrofracturing

Under a Science & Technology project in the year 2000, the National Institute of Rock Mechanics carried out hydrofracturing tests at Tandsi and Thesgora mines of Western Coalfields Ltd. The objective of this project was restricted to study the redistribution of stresses due to multiple mine openings and local tectonics like faults. Hydrofracturing stress measurements were conducted in shale and sandstone. These studies had given a fair idea about the validity of the Hydrofracturing experiments in porous rocks like sandstone. The pressure-time plots at Tandsi mines show a sharp peak at the breakdown pressure, whereas at Thesgora mines, the peak of the breakdown pressure was blunt, and the required shut-in pressure value could not be obtained to calculate the stress parameters. This was due to the occurrence of coarse-grained sandstone at Thesgora mines as compared to the carbonaceous shale and fine-grained sandstone at the Tandsi mines [44]. This was another example to show that the hydrofracture method can be applied in slightly porous rock-like shale but not in sandstone.

Liquid dissipation in hydrofracturing is not only linked with liquid dissipating into pores. If the liquid quantity is of higher amounts [45], the liquid dissipation in pores will be at a greater extent. So, the liquid flow must be more viscous and high flow in nature [46] (Fig. 2). The higher liquid flow rate is essential to initiate the moment in hydrofracturing by yielding lesser liquid dissipation into pores. But with extreme overpressure and pore-water pressure, this technique cannot be applied. At this instant, the fracturing process may not be successful. It will intend to create additional stress conditions by re-orientation of fractures [47] (Fig. 3). In the other case of fracturing, pores will be left open until there is a pressure drop. If there is any reduction in pressure, the fracturing process ends [48].

The quantity of liquid during hydrofracturing and associated losses depend on the rock's mechanical parameters and characteristics of liquid [49]. Hence, it is essential to study much more in detail about the liquid injection rate during hydrofracturing, the causes of liquid dissipation, and re-orientation. In some cases, changing the flow rate may often put some light on the reasons for re-orientation [50]. Due to the above reasons, various approaches need to be explored to trace out the dissipation part in different states and conditions. This may be effective in substituting the situation, which may help in finding possible solutions for the current problem.

Nevertheless, the experience in these mines has indicated that the hydrofracturing method can be used as a quick, reliable, and cost-effective means of understanding the in-situ stress field in coal mines, provided some drawbacks and limitations in the procedure of the measurements are properly addressed [51]. As more and more coal mines are facing roof problems because of the influence of stresses, the hydrofracturing method can be utilized

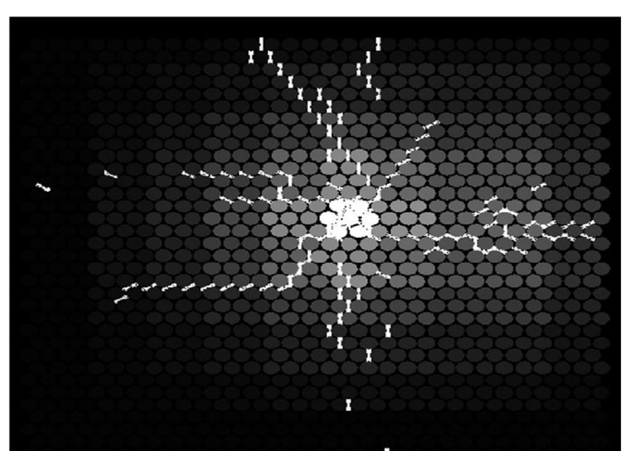

Fig. 2. Hydrofracturing test with liquid flow rate (1–8 L per minute) in permeable rocks.

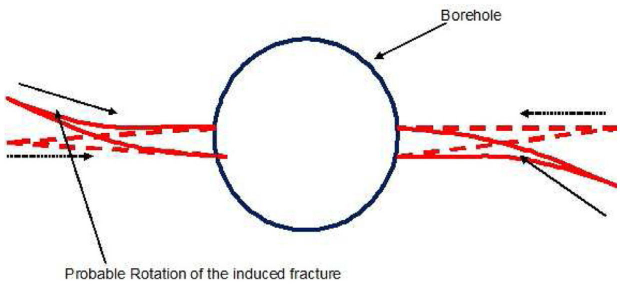

Fig. 3. Hydrofracturing test with a higher flow rate in permeable rocks.

quite effectively and economically to understand both in-situ stresses (deep inside the roof) and induced stresses (at the immediate roof) [52].

3. Hydrofracturing using viscous fluid

During hydrofracturing in sandstone, the non-viscous fluid like water is associated not only with liquid dissipation into pores but also the fracture opening, which tends to increase the volume of fluid loss. This loss also depends on the ability of the fluid to flow through the rock mass. Hence, the fluid must be selected on the viscosity rate.

In the case of flow rate in viscous fluid, it should be kept in such a way that from the moment of initiation of fracturing, it must yield minimum fluid loss into pores. But at this point, it should be taken care that the extreme pore pressures, and increase in flow rate, fracture should not take abnormal rotation with respect to the trend of pre-existing fractures/joints. This is studied and discussed in 7.0. An experimental study is carried out by conducting hydrofracturing tests in the field at certain depths where sandstone occurs. A hydrofracturing simulation is run on the cores obtained from the same depths of measurement. This has been tested with different flow rates in the laboratory with different confining pressures (horizontal and vertical).

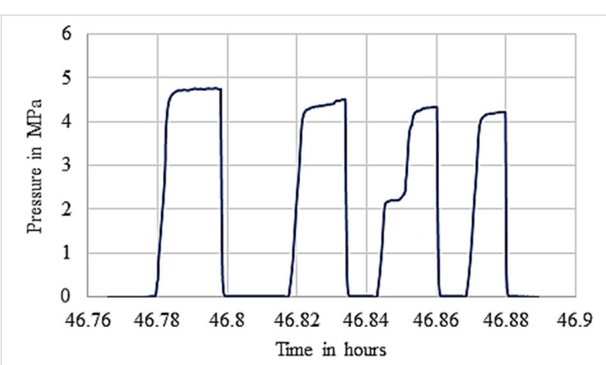

Fig. 4. Pressure vs time graph in case of SAE 10 motor oil.

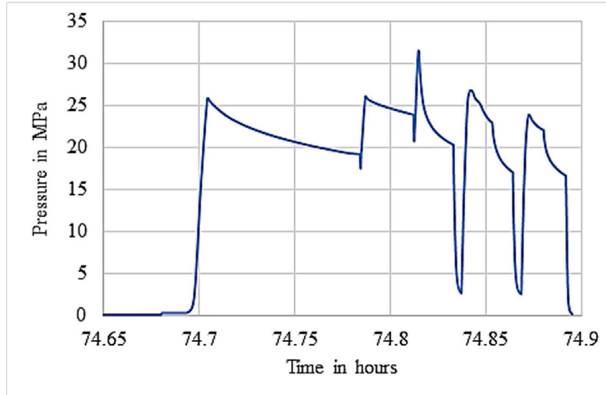

Fig. 5. Pressure vs time graph in case of ISO VG 320 oil.

ISO VG 320 oil of viscosity 0.27 Pa-second is used in this study for conducting hydrofracturing tests by running simulations in the lab on sandstone core samples. The validity of less viscosity liquid fluids like SAE 10 motor oil of viscosity 0.085 to 0.14 Pa-second is answerable in rock formations with porosity of much high porosity [53]. SAE 30 motor oil of viscosity from 0.42 to 0.65 Pa-second and ISO VG 460 of viscosity 0.39 Pa-second could not be able to open the pores, hence unable to obtain the breakdown pressures. Lesser flow rates of 0.0000005 m^3/s to 0.000001 m^3/s are usually applied as nominal flow rates depending on the extent, length of test zone and porosity [54]. There is no set of injection rate that can be fixed in prior [55]. Hence, pumping shall continue until a breakdown or shut-in is attempted. If not, the flow rates of 0.000001–0.0000015 m^3/s are kept as compliant in such case [56].

The fluid viscosity and flow rate depend on the properties of the rock mass. In a Science and technology project, the National Institute of Rock Mechanics carried out a series of tests at Shanti Kani mine, Singareni Collieries Company Limited, Telangana. The fluid of different viscosities was used on sandstone. In first trial viscous fluid of 0.085–0.140 Pa-second (SAE 10 motor oil) was applied. However, the fluid dissipated into the

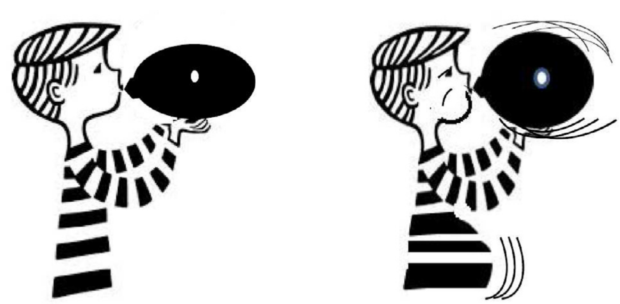

Fig. 6. Balloon phenomenon.

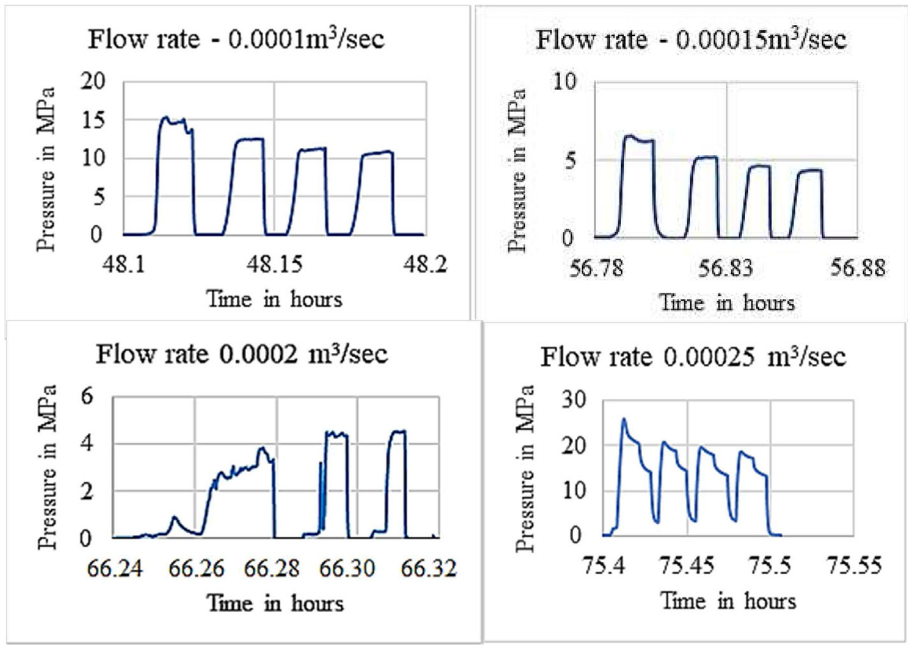

Fig. 7. Pressure vs time record for 0.0001 m^3/s to 0.00025 m^3/s injection rate.

pores, and the required pressure could not be reached. The instantaneous shut-in pressure corresponding to the quasi-static equilibrium state could not be reached. Hence, low viscous fluids of less than 0.2 Pa-second are found to be not suitable [57].

Later, viscous fluid of more than 0.3 Pa-second (SAE 30 motor oil) was used. In this case, the required pressure could not be built due to high viscosity in nature; hence pore pressure could not be built during fracturing. Finally, ISO VG 320 oil of viscosity 0.25–0.27 Pa-second was used. At that stage, the injection pressure was increased gradually by step flow rate (0.0000005 m^3/s, 0.000001 m^3/s and 0.0000015 m^3/s). There, the pre-existing fracture

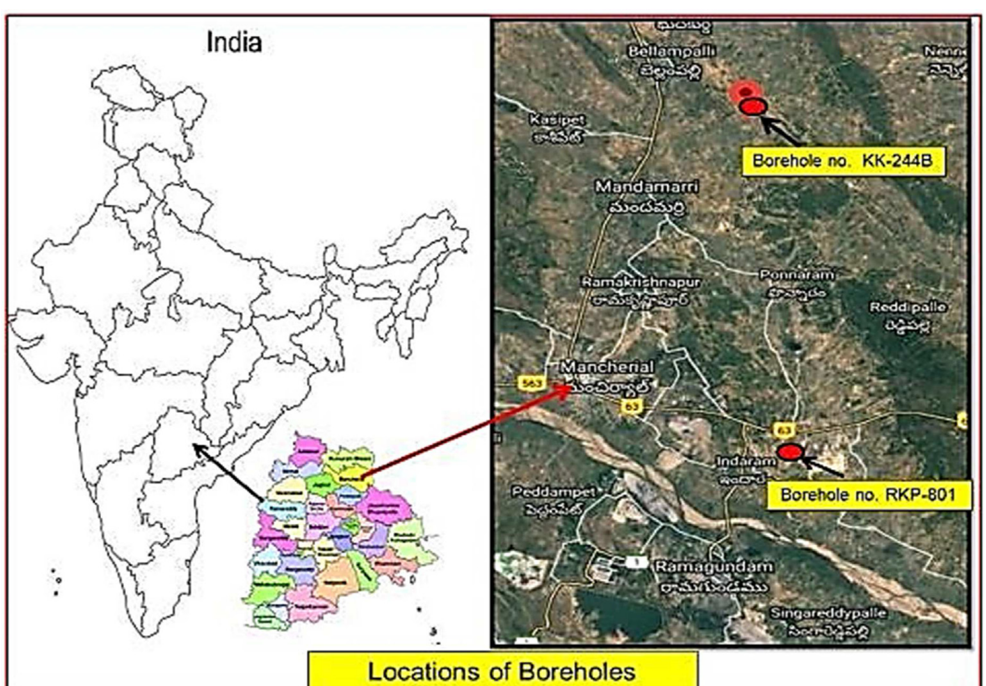

Fig. 8. Location of experimental sites.

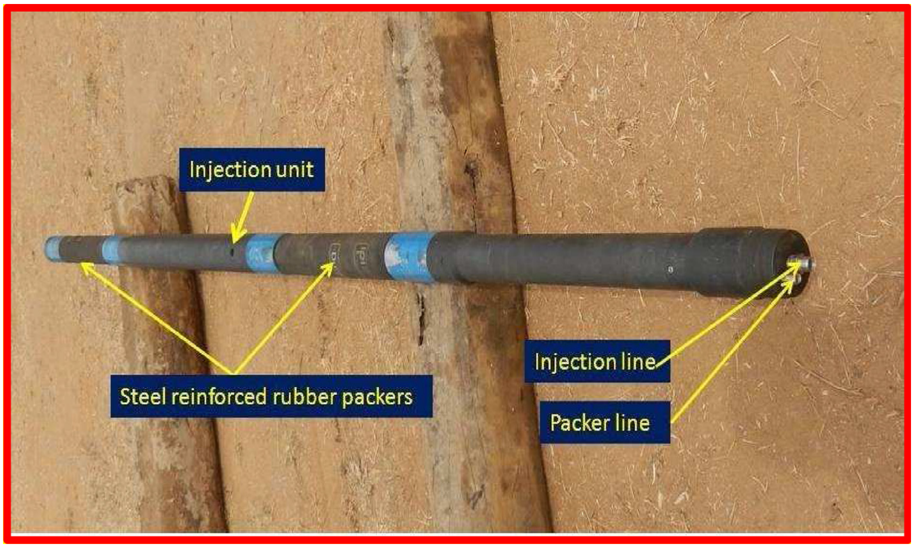

Fig. 9. Straddle packer system.

Fig. 10. Deephole hydrofrac system.

gets opened by subsequent two to three refract cycles were conducted followed by pump shut-off. The backflow was observed by short valve closures during venting (Figs. 4 and 5). Fluid viscosity of 0.2–0.3 Pa-second develops the required pressure in sandstone [57].

Fig. 11. Data acquisition system.

Fig. 12. Acoustic borehole televiewer logging system.

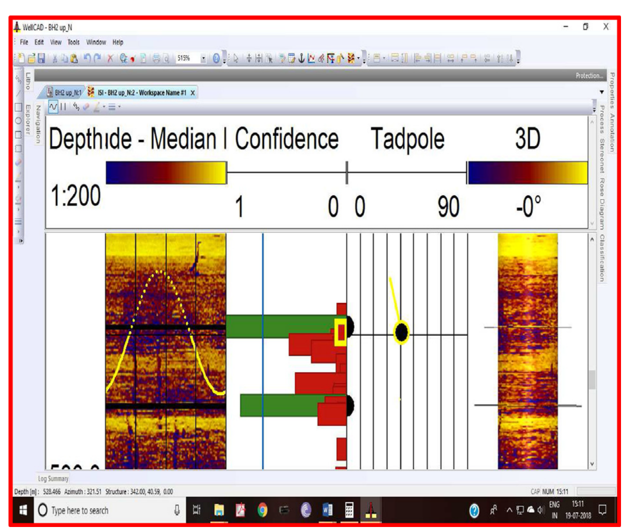

Fig. 13. Fracture trace obtained in BH No. RKP-801 depth 527.5 m.

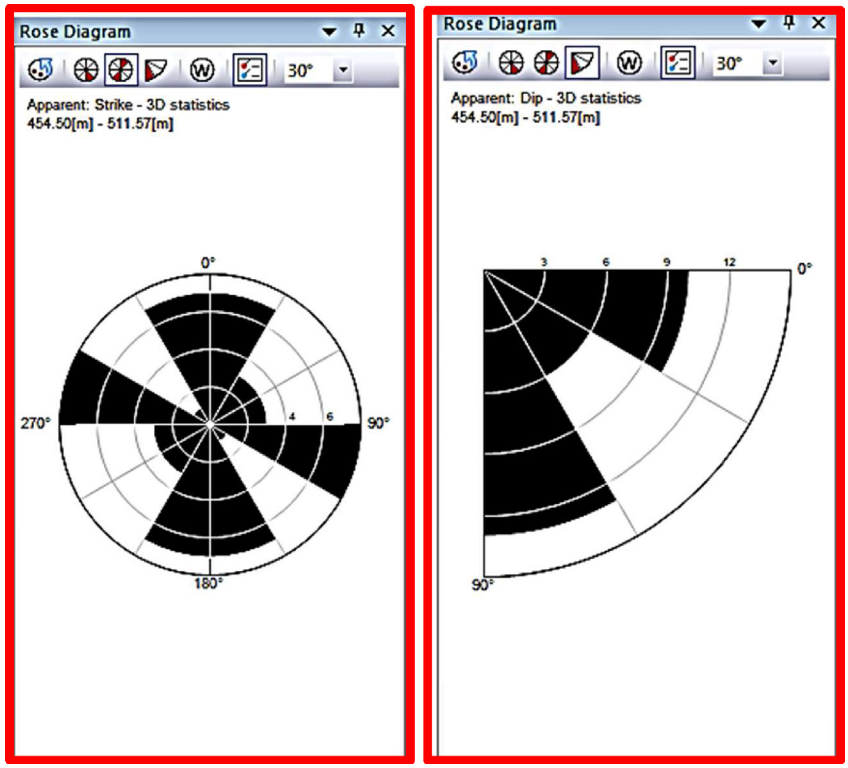

Fig. 14. Rose diagram representing major joint sets in borehole KK-244B.

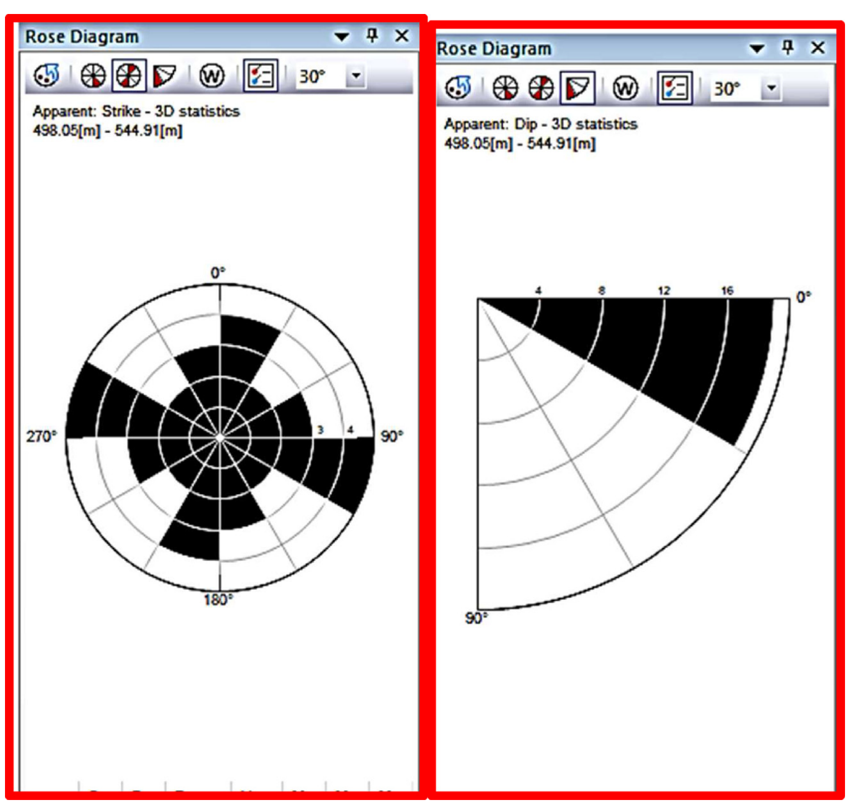

Fig. 15. Rose diagram representing major joint sets in borehole RKP-801.

Table 1. Results of the Mandamarri shaft block.

Parameters	Results
S_v	12.17
Major horizontal principle stress (S_H) in MPa	12.44
Minor horizontal principle stress (S_h) in MPa	6.22
Major horizontal principle stress direction	40°
$K = S_H/S_v$	1.02

Table 3. Results of the RKNT Dipside block.

Parameters	Results
S_v	12.80
Major horizontal principle stress (S_H) in MPa	17.79
Minor horizontal principle stress (S_h) in MPa	8.89
Major horizontal principle stress direction	20°
$K = S_H/S_v$	1.39

4. Hydrofracturing using high flow rate technique

The bloating phenomenon is the best example for explaining the high flow rate technique in hydrofracturing. A punctured balloon is blown up using different air pressures. It gets bloated only if air insertion is more than air release pressure through the puncture pore. So, the rate of airflow needs to be increased to keep up the balloon gets bloated (Fig. 6). A similar principle is adopted here in hydrofracturing in sandstone [58].

Byerlee (1975), in his study, showed that in the sedimentary strata under confined pressures, hydrofracturing may give better results. Shear or tensile stresses generated due to pore pressures are in controlled phenomenon [59]. A series of tests were conducted at different depths in the deep borehole of 600 m depth. The investigations were taken part at virgin coal blocks of Mandamarri shaft block and Ravindra Khani New Technology dipside block of Bellampalli coal belt, Singareni Collieries Company Limited, Telangana. Flow rates starting from 0.0001 m^3/s to 0.00025 m^3/s are applied. The shut-in pressure was obtained at 0.00025 m^3/s (Fig. 7). At lesser flow rates, pore pressure could not be able to build during fracturing. Pressure gets dissipated along porous sandstone [60]. Hence, fluid flow was gradually raised in stages to observe the pore pressures passing the shear strength and tension crack gets developed [61].

5. Hydrofracturing conducted in field using high flow rate technique

Tests were conducted from 472.5 to 517.55 m depth in BH. No. KK244B of Mandamarri shaft block and 520.5–544.5 m depth in BH. No. RKP-801 of Ravindra Khani New Technology (RKNT) dipside block of Bellampalli coal belt, Singareni Collieries Company Limited, Telangana (Fig. 8). The hydrofracturing system with steel wire reinforced packers of 70 mm Outer Diameter (Fig. 9) was used. The length of each packer is 635 mm. This is imported from Australia and designed by IPI (Inflatable Packers International). The test interval length is 350 mm.

Two number high-pressure hoses (ø 3/8”, working pressure 78 MPa/burst pressure 280 MPa and ø ¼”, working pressure 72 MPa/burst pressure 288 MPa) used for water injection and packer inflation. The pump working pressure is 50 MPa and nominal flow ranges from one to sixteen litres per minute (Fig. 10) is used. The pump is driven by a 3-phase 440-V AC electric induction motor. Pressure is controlled by a sophisticated flow control system. Digitally the information is collected in memory gauge which is stored-fitted in the instrument and thereby data can be retrieved for analysis in mean time using laptop computer with the help of sophisticated system for decrypting data from board – Pico logger (Fig. 11).

High-resolution Acoustic Borehole Televiewer logging is used to map the geological formations in the borehole (Fig. 12). The data is recorded and processed in sophisticated Well CAD software. The software Well CAD incorporates the opened/induced fracture trace raw data obtained from the Acoustic borehole televiewer tool (Fig. 13).

6. Results of hydrofracturing test

Results are determined under two conditions:

i) Topography of the study area.

Table 2. Field data obtained at Mandamarri shaft block.

BH. No.	Depth in m	Fracture inclination (degrees, 0° horizontal and 90° vertical)	Fracture strike (N-E, degrees)	Shut-in pressure (P_{si} in MPa)
KK-244B	472.5	80.20	330.19	11.85
	489.5	82.89	239.88	7.25
	496.5	88.79	185.41	12.19

Table 4. Field data obtained at RKNT Dipside block.

BH. No.	Depth in m	Fracture inclination (degrees, 0° horizontal and 90° vertical)	Fracture strike (N-E, degrees)	Shut-in pressure (P_{si} in MPa)
RKP-801	527.5	40.59	252.00	15.92
	533.5	56.61	121.78	21.03
	544.5	70.94	111.88	11.29

ii) Anisotropy of the rock mass [62].

The data is analysed using the code program *GENSIM.* It is a sophisticated software, based on stress inversion technique, that solves by carrying out iterations by the root of mean squares method to determine the minor principle horizontal stress magnitude and direction of the major principle horizontal stress using the below formulae [63]:

$$S_h = (P_{si} - n^2 \cdot S_V)/(m^2 + l^2 \cdot S_H/S_h)$$

Where, l, m, n are the cosines of the directions of the induced or pre-existing fractures, S_v is vertical stress, S_H is major horizontal principle stress, and S_h is minor principle horizontal stress.

From the sonic log, the major joint sets are obtained. It is oriented from 454 m to 511 m in borehole KK-244B in E–W direction, dipping 80–90° and in borehole RKP-801 from 498 m to 544 m, the major joint sets are aligned in E-W direction, dipping 20–30° (Figs. 14 and 15).

The results were tabulated (Tables 1 and 3) from data in Tables 2 and 4.

Fig. 16. Fraclab hydraulic fracture test system.

7. Hydrofracturing simulation study in laboratory on cores

A simulation study is run on cores (54.7 mm diameter) where hydrofracturing tests done in field (i.e., cores obtained from KK-244B at 472.5–496.5 m and RKP-801 at 527.5–544.5 m) to compare the effects of fracture propagation and delineation characteristics. Fraclab hydraulic fracture test system manufactured by Floxlab is used for running simulations on core samples subjected to different stress states (Fig. 16). Stress ratios of horizontal to vertical stress have been maintained from 0.5 to 2.5.

The test system carries out hydraulic fracture experiments with micro-seismic activity monitoring under various triaxial stress states. The device consists of a triaxial stress cell equipped with an acoustic emission monitoring system. Four servo-controlled syringe pumps are used to control confining (70 MPa max.), axial (424 MPa max.), pore (70 MPa max.) and fracturing fluid pressures (70 MPa). The apparatus determines specimen breakdown pressure at given confining and pore pressures, after which the tensile strength and frac-coefficient are computed. The acoustic emission (AE) monitoring system allows the characterization of fracture growth during geotechnical studies.

In this experiment, fluid flow is maintained in three modes: 0.0000005 m^3/s, 0.000001 m^3/s and 0.0000015 m^3/s. The viscosity of fluid 0.25 to 0.27 Pa-second is applied for hydrofracturing. The stress

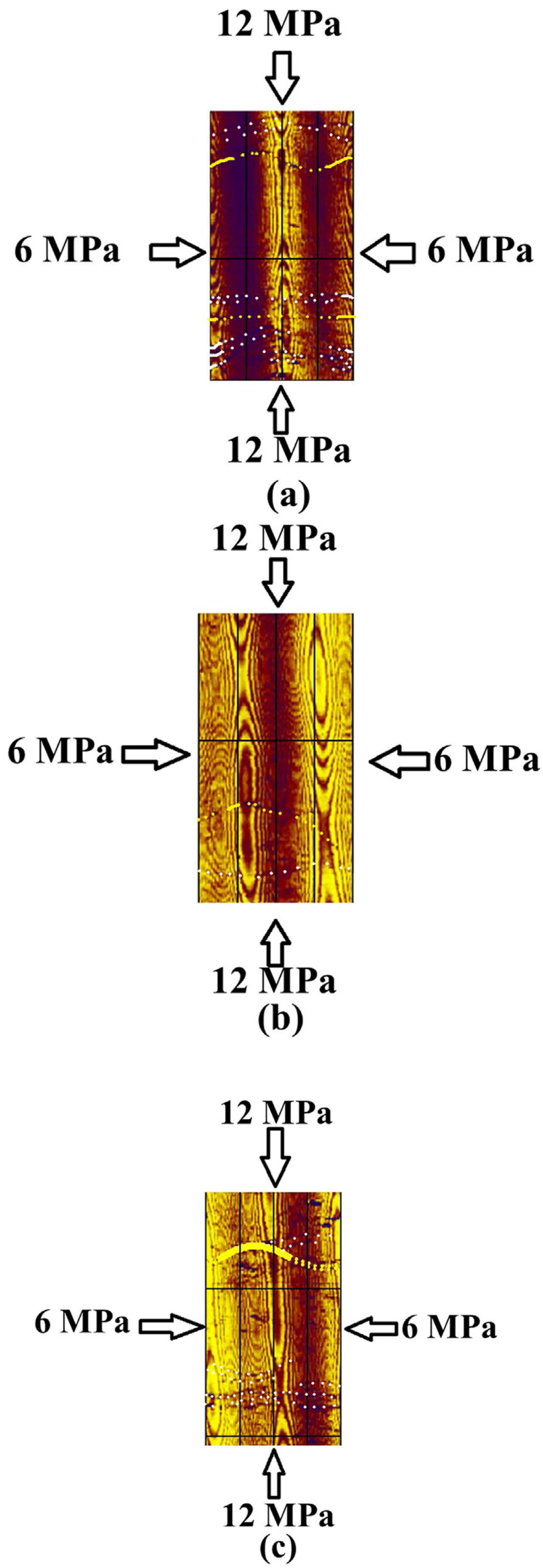

Fig. 17. Propagation of fracture in case of axial vs confining pressure stress ratio of 0.5 and variable fluid flow range (i.e., (a) 0.0000005 m^3/s, (b) 0.000001 m^3/s and (c) 0.0000015 m^3/s).

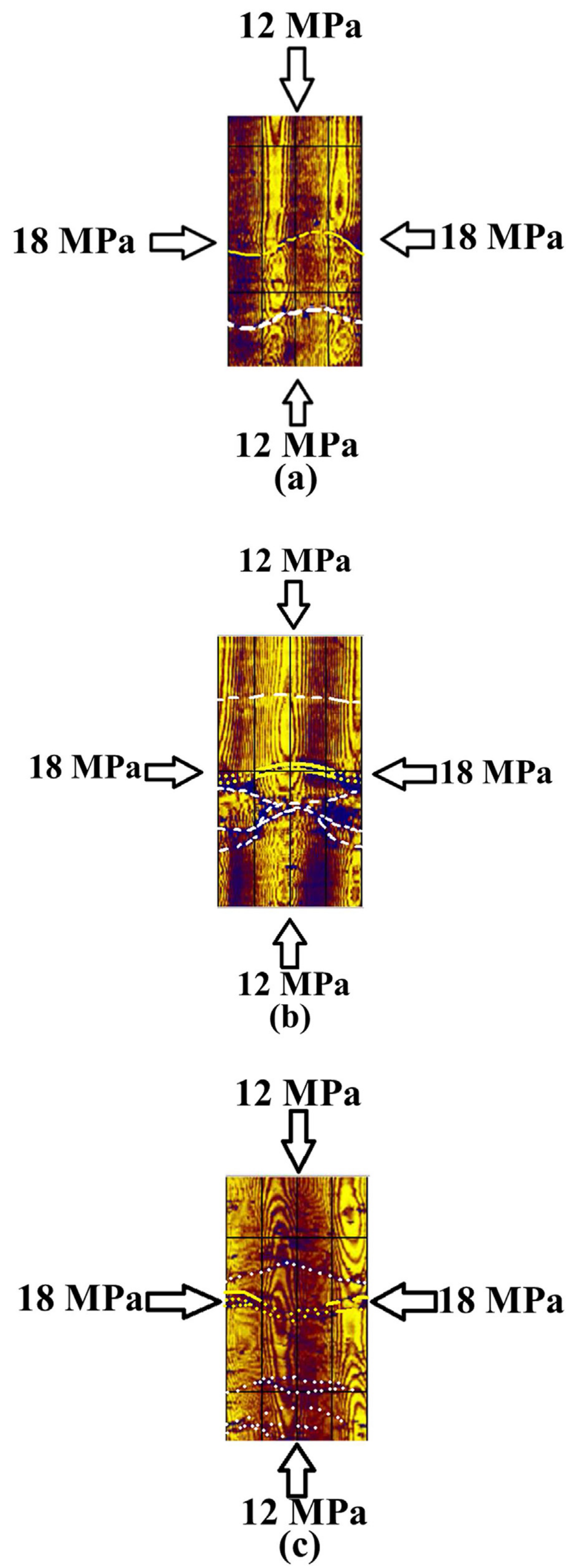

Fig. 18. Propagation of fracture in case of axial vs confining pressure stress ratio of 1.5 and variable fluid flow range (i.e., (a) 0.0000005 m^3/s, (b) 0.000001 m^3/s and (c) 0.0000015 m^3/s).

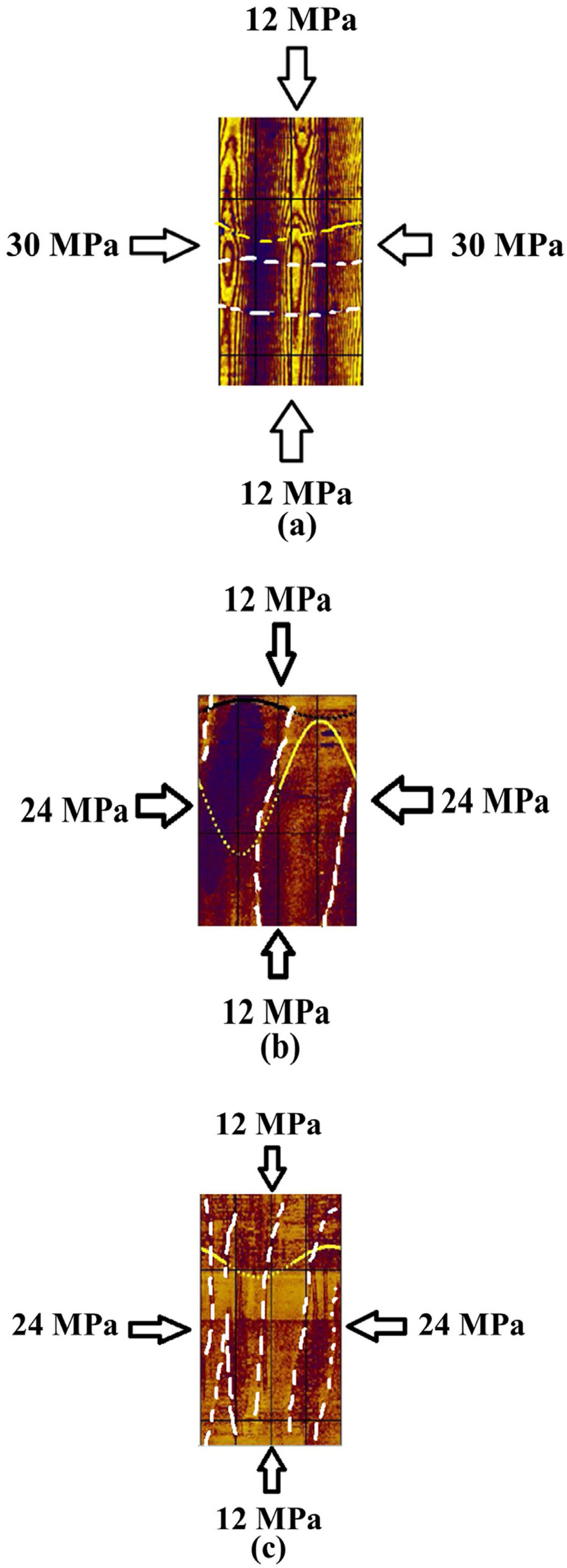

Fig. 19. Propagation of fracture in case of axial vs confining pressure stress ratio of 2.0 and variable fluid flow range (i.e., (a) 0.0000005 m^3/s, (b) 0.000001 m^3/s and (c) 0.0000015 m^3/s).

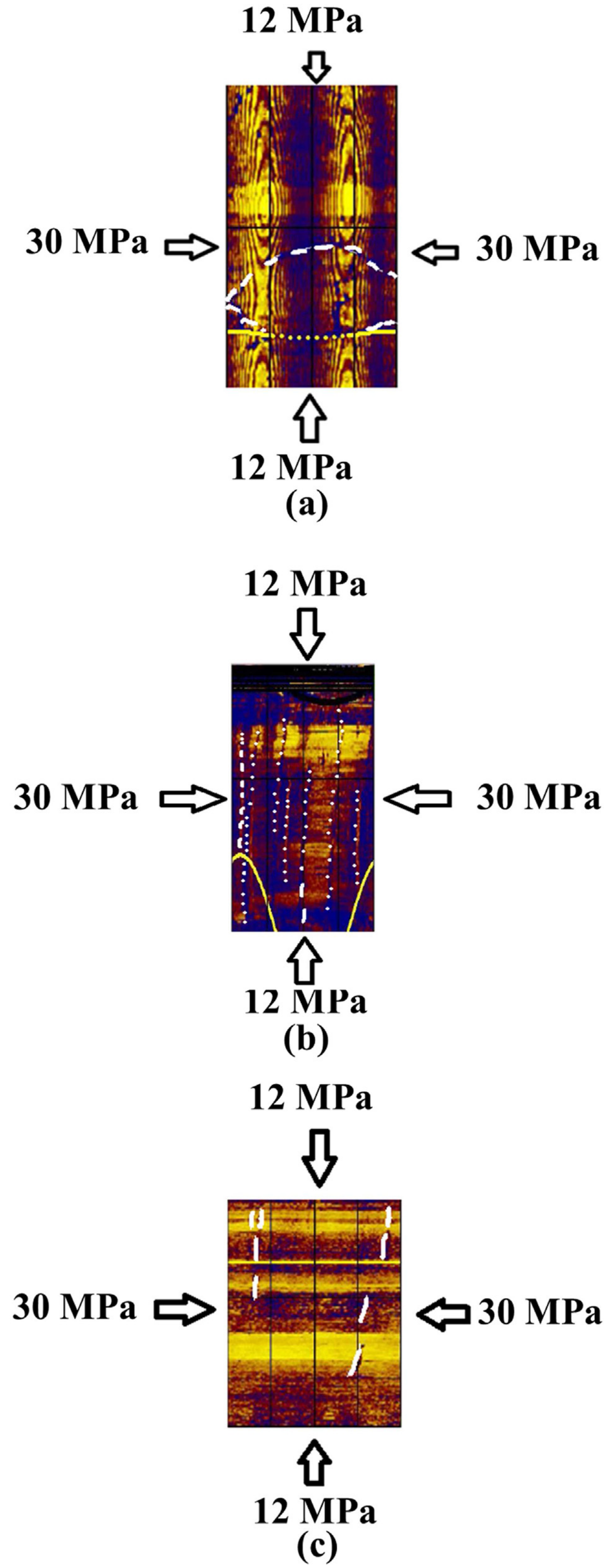

Fig. 20. Propagation of fracture in case of axial vs confining pressure stress ratio of 2.5 and variable fluid flow range (i.e., (a) 0.0000005 m^3/s, (b) 0.000001 m^3/s and (c) 0.0000015 m^3/s).

Table 5. Results of the Mandamarri shaft block in case of axial vs confining pressure stress ratio of 0.5 and variable fluid flow range (i.e., (a) 0.0000005 m^3/s, (b) 0.000001 m^3/s and (c) 0.0000015 m^3/s).

Parameters	Results
S_v	12
Major horizontal principle stress (S_H) in MPa	22.07
Minor horizontal principle stress (S_h) in MPa	11.03
Major horizontal principle stress direction	N 120°
$K = S_H/S_v$	1.83

ratios are observed from 0.5 to 2.5, i.e., axial (12 MPa) vs confining pressures (6, 18, 24, 30 MPa). A pore pressure of 4 MPa is maintained throughout the experiment because the same is observed during observation in the field from the downhole piezo. Results show that at lower stress ratios of 0.5 and 1.5, fluid flow of 0.0000005 m^3/s, 0.000001 m^3/s and 0.0000015 m^3/s, there is not much change in trend in fracture propagation (Figs. 17 and 18). It tends along the pre-existing fractures. But when the stress ratios increased from 2 to 2.5, with flow rates of 0.000001 m^3/s to 0.0000015 m^3/s, the trend of fracture propagation is across the maximum loading direction (Figs. 19 and 20). The propagation trend is in yellow & fractures are in white streaks.

This change in trend is due to a change in stress state, which plays a crucial role in fracture propagation. Hence, now the concern is with fluid flow and stress state that need to be addressed. From the above study, a flow rate of 0.0000005 m^3/s to 0.0000015 m^3/s is feasible in a stress state of 0.5–1.5. The stress state of 2–2.5 is not found feasible, when the flow rate is increased to 0.000001 m^3/s and 0.0000015 m^3/s. The fracture trend is along the confining pressure. The core sample at depth shows the pre-existing fractures are parallel to the axial load. This suggests that the fluid flow at 0.0000005 m^3/s did not affect the fracture trend, but when the flow increased to 0.000001 m^3/s and 0.0000015 m^3/s, the fracture trend gets delineated. Hence, the suitable flow falls between 0.0000005 m^3/s and 0.0000008 m^3/s at all stress states.

The stress results obtained from the laboratory studies also pour much light on how the fracture delineation occurs, and the major principle stress

Table 6. Lab data obtained in case of axial vs confining pressure stress ratio of 0.5 and variable fluid flow range (i.e., (a) 0.0000005 m^3/s, (b) 0.000001 m^3/s and (c) 0.0000015 m^3/s) at Mandamarri shaft block.

BH No.	Depth in m	Fracture inclination (degrees, 0° horizontal and 90° vertical)	Fracture strike (N-E, degrees)	Shut-in pressure (P_{si} in MPa)
KK-244B	470.5	86.2	306.2	11.06
	487.5	84.8	271.3	13.4
	494.5	60.6	145	13.07

Table 7. Results of the RKNT dipside block in case of axial vs confining pressure stress ratio of 0.5 and variable fluid flow range (i.e., (a) 0.0000005 m^3/s, (b) 0.000001 m^3/s and (c) 0.0000015 m^3/s).

Parameters	Results
S_v	12
Major horizontal principle stress (S_H) in MPa	25.6
Minor horizontal principle stress (S_h) in MPa	17.06
Major horizontal principle stress direction	N 120°
$K = S_H/S_v$	2.13

Table 9. Results of the Mandamarri shaft block in case of axial vs confining pressure stress ratio of 1.5 and variable fluid flow range (i.e., (a) 0.0000005 m^3/s, (b) 0.000001 m^3/s and (c) 0.0000015 m^3/s).

Parameters	Results
S_v	12
Major horizontal principle stress (S_H) in MPa	15.82
Minor horizontal principle stress (S_h) in MPa	10.55
Major horizontal principle Stress direction	N 130°
$K = S_H/S_v$	1.31

Table 8. Lab data obtained in case of axial vs confining pressure stress ratio of 0.5 and variable fluid flow range (i.e., (a) 0.0000005 m^3/s, (b) 0.000001 m^3/s and (c) 0.0000015 m^3/s) at RKNT dipside block.

BH No.	Depth in m	Fracture inclination (degrees, 0° horizontal and 90° vertical)	Fracture strike (N-E, degrees)	Shut-in pressure (P_{si} in MPa)
RKP-801	525.5	89.4	275.1	18.0
	531.5	84.9	116.5	17.8
	542.5	87.3	337.3	20.0

Table 10. Lab data obtained in case of axial vs confining pressure stress ratio of 1.5 and variable fluid flow range (i.e., (a) 0.0000005 m^3/s, (b) 0.000001 m^3/s and (c) 0.0000015 m^3/s) at Mandamarri shaft block.

BH No.	Depth in m	Fracture inclination (degrees, 0° horizontal and 90° vertical)	Fracture strike (N-E, degrees)	Shut-in pressure (P_{si} in MPa)
KK-244B	471.5	77.8	119.28	13.6
	488.5	83.42	25.21	14.0
	495.5	83.57	76.61	13.0

Table 11. Results of the RKNT dipside block in case of axial vs confining pressure stress ratio of 1.5 and variable fluid flow range (i.e., (a) 0.0000005 m^3/s, (b) 0.000001 m^3/s and (c) 0.0000015 m^3/s).

Parameters	Results
S_v	12
Major horizontal principle stress (S_H) in MPa	17.15
Minor horizontal principle stress (S_h) in MPa	11.43
Major horizontal principle stress direction	N 120°
$K = S_H/S_v$	1.42

Table 15. Results of the RKNT dipside block in case of axial vs confining pressure stress ratio of 2.0 and variable fluid flow range (i.e., (a) 0.0000005 m^3/s, (b) 0.000001 m^3/s and (c) 0.0000015 m^3/s).

Parameters	Results
S_v	12
Major horizontal principle stress (S_H) in MPa	25.74
Minor horizontal principle stress (S_h) in MPa	17.16
Major horizontal principle stress direction	N 20°
$K = S_H/S_v$	2.14

Table 12. Lab data obtained in case of axial vs confining pressure stress ratio of 1.5 and variable fluid flow range (i.e., (a) 0.0000005 m^3/s, (b) 0.000001 m^3/s and (c) 0.0000015 m^3/s) at RKNT dipside block.

BH No.	Depth in m	Fracture inclination (degrees, 0° horizontal and 90° vertical)	Fracture strike (N-E, degrees)	Shut-in pressure (P_{si} in MPa)
RKP-801	526.5	89.4	265.3	13.8
	532.5	72.8	153.4	13.5
	543.5	75.1	181.9	14.6

Table 13. Results of the Mandamarri shaft block in case of axial vs confining pressure stress ratio of 2.0 and variable fluid flow range (i.e., (a) 0.0000005 m^3/s, (b) 0.000001 m^3/s and (c) 0.0000015 m^3/s).

Parameters	Results
S_v	12
Major horizontal principle stress (S_H) in MPa	32.23
Minor horizontal principle stress (S_h) in MPa	21.49
Major horizontal principle stress direction	N 20°
$K = S_H/S_v$	2.68

orientation is altering when the stress ratios are changed from 0.5, 1.5, 2 and 2.5 (Tables 5−20). The fracture traces obtained in the field and the lab are compared. There is a huge difference of 80°−300° observed when the stress ratios changed from 1.5 to 2.0 and 2.5 (Table 21).

It is found to be evident that the re-orientation of fracture is caused due to stress ratio 2 and 2.5, and the flow rate is increased from 0.000001 m^3/s to

Table 14. Lab data obtained in the case of axial vs confining pressure stress ratio of 2.0 and variable fluid flow range (i.e., (a) 0.0000005 m^3/s, (b) 0.000001 m^3/s and (c) 0.0000015 m^3/s) at Mandamarri shaft block.

BH No.	Depth in m	Fracture inclination (degrees, 0° horizontal and 90° vertical)	Fracture strike (N-E, degrees)	Shut-in pressure (P_{si} in MPa)
KK-244B	473.5	90	46	24.56
	490.5	90	86	21.95
	497.5	90	130	27.68

Table 16. Lab data obtained in case of axial vs confining pressure stress ratio of 2.0 and variable fluid flow range (i.e., (a) 0.0000005 m^3/s, (b) 0.000001 m^3/s and (c) 0.0000015 m^3/s) at RKNT dipside block.

BH No.	Depth in m	Fracture inclination (degrees, 0° horizontal and 90° vertical)	Fracture strike (N-E, degrees)	Shut-in pressure (P_{si} in MPa)
RKP-801	528.5	24.11	172.85	21
	534.5	90	108.50	20.24
	545.5	31.19	144.94	21.42

Table 17. Results of the Mandamarri shaft block in case of axial vs confining pressure stress ratio of 2.5 and variable fluid flow range (i.e., (a) 0.0000005 m^3/s, (b) 0.000001 m^3/s and (c) 0.0000015 m^3/s).

Parameters	Results
S_v	12
Major horizontal principle stress (S_H) in MPa	32.5
Minor horizontal principle stress (S_h) in MPa	21.67
Major horizontal principle stress direction	N 20°
$K = S_H/S_v$	2.70

0.0000015 m^3/s. Also the major principle stress orientation is re-orienting when the stress ratio is changed from 1.5 to 2 and 2.5 and the flow rate is being increased from 0.000001 m^3/s to 0.0000015 m^3/s. In Tables 5, 7, 9 and 11. The principle stress orientation is ranging from 120° to 130°. The stress orientation obtained in Tables 13, 15, 17 and 19 is 20°. This is similar to field results.

Table 18. Lab data obtained in case of axial vs confining pressure stress ratio of 2.5 and variable fluid flow range (i.e., (a) 0.0000005 m^3/s, (b) 0.000001 m^3/s and (c) 0.0000015 m^3/s) at Mandamarri shaft block.

BH No.	Depth in m	Fracture inclination (degrees, 0° horizontal and 90° vertical)	Fracture strike (N-E, degrees)	Shut-in pressure (P_{si} in MPa)
KK-244B	474.5	33.35	4.59	20
	491.5	65.92	173.81	22.5
	498.5	40.98	26.47	21.5

Table 19. Results of the RKNT dipside block in case of axial vs confining pressure stress ratio of 2.5 and variable fluid flow range (i.e., (a) 0.0000005 m^3/s, (b) 0.000001 m^3/s and (c) 0.0000015 m^3/s).

Parameters	Results
S_v	12
Major horizontal principle stress (S_H) in MPa	28.23
Minor horizontal principle stress (S_h) in MPa	18.82
Major horizontal principle stress direction	N 20°
$K = S_H/S_v$	2.35

8. Conclusions

In recent days, Hydrofracturing test had become widely used method for measuring in situ stress at deeper extents. This method has fewer assumptions [64]. However, in some cases, it is not fully understood where the problem arises during application [65]. In sandstone, due to high porosity, it is difficult to arrive at results and has shown

Table 20. Lab data obtained in case of axial vs confining pressure stress ratio of 2.5 and variable fluid flow range (i.e., (a) 0.0000005 m^3/s, (b) 0.000001 m^3/s and (c) 0.0000015 m^3/s) at RKNT dipside block.

BH No.	Depth in m	Fracture inclination (degrees, 0° horizontal and 90° vertical)	Fracture strike (N-E, degrees)	Shut-in pressure (P_{si} in MPa)
RKP-801	529.5	90	58.73	23
	535.5	70.95	52.94	20.5
	546.5	67.78	150.47	23.5

Table 21. Fracture traces obtained from field and laboratory studies.

BH No.	Depth in m	Field	Lab			
		Fracture strike (N-E, Deg)	Stress ratios			
			0.5	1.5	2	2.5
			Fracture strike (N-E, Deg)			
KK-244B	472.5	330.19	306.2	119.28	46	4.59
	489.5	239.88	271.3	25.21	86	173.81
	496.5	185.41	145	76.61	130	26.47
RKP-801	527.5	252.00	275.1	265.3	172.85	58.73
	533.5	121.78	116.5	153.4	108.50	52.94
	544.5	111.88	337.3	181.9	144.94	150.47

legible [66]. Other methods do make it out, but due to the complexity and nature of rock formation, one must modify and identify the solutions for the current problems.

From the study, it is found that the fracture delineation and major principle stress re-orientation phenomenon is causing in sandstone. This is due to the stress ratio present (2 and 2.5) and the high flow rates (0.000001 m^3/s to 0.0000015 m^3/s). The stress results obtained in the field are re-oriented (Tables 1 and 3). It is found matching the results obtained in simulation studies (Tables 13, 15, 17 and 19).

The ISO VG 320 oil is applied to obtain shut-in pressures using a normal flow rate (0.0000005 m^3/s to 0.0000008 m^3/s) in a laboratory simulation. The stress re-orientation is stopped in a stress ratio of 0.5 and 1.5. The fracture traces obtained are along the pre-existing joints (Tables 6, 8, 10 and 12). The major joint sets obtained from the sonic log represents that in both boreholes, they are oriented in E–W direction (Figs. 14 and 15), which is similar to the major principle stress direction 120°–130° obtained from laboratory simulation (Tables 5, 7, 9 and 11). The major joints are the indications for the paleo stress conditions, which are act along major principle stress direction and are caused by it.

Conflicts of interest

The authors declare no conflicts of interest.

Ethical statement

The authors state that the research was conducted according to ethical standards.

Funding body

This research was funded by Ministry of Coal, Government of India under supervision of Central Mine Planning and Design Institute, grant number MT-165.

Acknowledgements

The authors are thankful to the Ministry of Coal and CMPDI for providing grants under S&T projects. The authors are also grateful to the management and executives at the test locations of M/s SCCL for their support and tireless efforts. The authors are also thankful for the support extended by M/s Floxlab. The authors are thankful to the Director of the National Institute of Rock Mechanics for providing suggestions & permitting to publish this paper.

References

[1] Satya Subrahmanyam D. Hydraulic fracturing in porous and fractured rocks. Emerging technologies in hydraulic fracturing and gas flow modelling. Intech Open 2022:57–91. https://doi.org/10.5772/intechopen.106552.

[2] Enever JR, Wooltorton BA. Experince with hydraulic fracturing as a means of estimating *in situ* stress in Australian coal basin sediments. Hydraulic fracturing stress measurements. Proceedings of a workshop December 1981:2–5.

[3] Baumgartner J, Rummel F. Experience with 'Fracture pressurization tests' as a stress measuring technique in a jointed rock mass. Int J Rock Mech Min Sci Geomech Abstr 1989;26: 661–71.

[4] Beugelsdijk LJL, Pater CJD, Sato K. Experimental hydraulic fracture propagation in a multi fractured medium. In: SPE 59419, presented at the 2000 SPE asia pacific conference. Yokohama: Japan; 2000.

[5] Bush D, Barton D. Application of small-scale hydraulic fracturing for stress measurements of bedded salt. Minneapolis, Minnesota, USA. Proceedings of the 2nd international workshop on Hydraulic fracturing stress measurements. 1988. p. 344–66.

[6] Gronseth JM, Key. Instantaneous shut-in pressure and its relationship to the minimum *in situ* stress. Hydraulic fracturing stress measurements. Proceedings of a workshop December 1981:2–5.

[7] Warpinski N. Determining the minimum in-situ stress from hydraulic fracturing through perforations. Minneapolis, Minnesota, USA. Proceedings of the 2nd international workshop on Hydraulic fracturing stress measurements. 1988. p. 800–40.

[8] John D, McLennan, Jean Claude. Do instantaneous shut-in pressure accurately represent the minimum principal stress. Hydraulic fracturing stress measurements. Proceedings of a workshop December 1981:2–5.

[9] Zhou J, Jin Y, Chen M. Experimental investigation of hydraulic fracturing in random natural fractured blocks. Int J Rock Mech Min Sci 2010;47:1193–9.

[10] Clarkson CR, Solano N, Bustin RM, Bustin AMM, Chalmers GRL, He L. Pore structure characterization of north American shale gas reservoirs using USANS/SANS, gas adsorption, and mercury intrusion. Fuel 2013;103:606–16.

[11] Haimson BC. Hydrofracturing stress measurements in the blue ridge belt of South Carolina. EOS 1976;57:289.

[12] Roegiers JC, McLennan JC, Schultz LD. *In situ* stress determination in northeastern Ohio, Proc, 23rd U.S. Symposium on Rock Mechanics. Berkeley, CA: University of California; 1982.

[13] McClure Mark, Kang Charles, Fowler Garrett. Optimization and design of next-generation geothermal systems created by multistage hydraulic fracturing. The Woodlands, Texas, USA. SPE hydraulic fracturing technology conference and exhibition. 2022. https://doi.org/10.2118/209186-MS.

[14] Bredehoeft JD, Wolff RG, Keys WS, Shuter E. Hydraulic fracturing to determine the regional in situ stress field, Piceance Basin, Colorado. Geol Soc Am Bull 1976;87:250–8.

[15] Haimson BC, Fairhurst C. *In situ* stress determination at great depth by means of hydraulic fracturing. Proceedings of 11th US symposium of rock mechanics. Berkeley: SME/AIME; 1970. p. 559–84.

[16] Haimson BC, Rummel F. Hydrofracturing stress measurements in the Iceland research drilling project drill hole at reydarfjordur, Iceland. J Geophys Res Solid Earth 1982; 87(B8):6631–49. https://doi.org/10.1029/JB087iB08p06631.

[17] Huang BX. Research on theory and application of hydraulic fracture weakening for coal–rock mass. Doctoral thesis. China University of Mining and Technology; 2008.

[18] Zhou J, Chen M, Jin Y, Zhang GQ. Analysis of fracture propagation behaviour and fracture geometry using a triaxial fracturing system in naturally fractured reservoirs. J Rock Mech Min Sci 2008;45:1143–52.

[19] Zhou J, Chen M, Jin Y, Zhang GQ. Experiment of propagation mechanism of hydraulic fracture in multi-fracture reservoir. J China Univ Petrol (Ed Nat Sci) 2008;32(4):51–4.

[20] Stephen H, Hickman M, Zoback D. The Interpretation of hydraulic fracturing pressure-time data for *in situ* stress determination. Hydraulic fracturing stress measurements. Proceedings of a workshop December 1981:2–5.

[21] Haimson BC, Fairhurst C. Initiation and extension of hydraulic fractures in rocks. September Soc Petrol Eng J 1967: 10–8.

[22] Jeffrey RG, Bunger A, Lecampion B, Zhang X, Chen ZR, As AV, Allison DP, Beer WD, Dudley JW, et al. Measuring hydraulic fracture growth in naturally fractured rock. In: SPE 124919, presented at the SPE annual technical conference and exhibition. New Orleans, USA: Louisiana; 2009.

[23] Cornet FH, Burlet D. Stress field determinations in France by hydraulic tests in boreholes. J Geophys Res 1992;97: 11829–49.

[24] Cornet FH, Valette B. *In situ* Stress determination from hydraulic test data. J Geophys Res 1984;97:11527–37.

[25] Doe T, Boyce G. Orientation of hydraulic fracturing in salt under hydrostatic and non-hydrostatic stresses. Minneapolis, Minnesota, USA. Proceedings of the 2nd international workshop on Hydraulic fracturing stress measurements. 1988. p. 366–93.

[26] Du CZ. Study on theoretics of hydraulic fracturing in coal bed and its applications. Doctoral thesis. China University of Mining and Technology; 2008.

[27] Haimson BC. Unpublished PhD thesis. In: Hydraulic fracturing in porous and nonporous rock and its potential for determining *in situ* stresses at great depth. University of Minnesota; 1968. p. 234.

[28] Rummel F, Jung R. Hydraulic fracturing stress measurements near the Hohenzollern-Graben-structure, SW Germany. Pure and Applied Geophysics PAGEOPH 1975;113: 321–30. https://doi.org/10.1007/bf01592921.

[29] Stephansson O. State of the art and future plans about hydraulic fracturing stress measurements in Sweden. Proceedings of Hydraulic fracturing stress measurements. Monterey, Washington. DC: National Academy Press; 1983. p. 260–7.

[30] Soliman MY, East L, Augustine J. Fracturing design aimed at enhancing fracture complexity. Barcelona, Spain. In: SPE 130043, presented at the SPE EUROPEC/EAGE annual conference and exhibition; 2010.

[31] Cheung LS, Haimson BC. Hydraulic fracturing stress measurements in intact and prefractured rock – a laboratory study. Minneapolis, Minnesota, USA. Proceedings of the 2nd international workshop on Hydraulic fracturing stress measurements. 1988. p. 542–83.

[32] Enever JR. Ten years experience with hydraulic fracture stress measurement in Australia. Minnesota: Proc. of the Second International Workshop on Hydraulic Fracture Stress Measurements; 1988. p. 1–92.

[33] Evans. Some problems in estimating horizontal stress magnitudes in thrust regimes. Proceedings of the second International Workshop on Hydraulic Fracturing stress Measurements 1988;–1:275.

[34] Haimson BC. A simple method for estimating in-situ stress at great depths. ASTM Spec. Tech. Publ. Field Testing and Instrumentation of Rock 1974;554:156–82.

[35] Kirsch EG. Die Theorie der Elastizität und die Bedürfnisse der Festigkeitslehre. Z Des Vereines Dtsch Ingenieure 1898; 42:797–807.

[36] Szymanski J, Harper T, Daly M. Application of hydrofracturing to the characterization of geologic conditions. Minneapolis, Minnesota, USA. Proceedings of the 2nd international workshop on Hydraulic fracturing stress measurements. 1988. p. 393–410.

[37] Wand Y, Miskimins JL. Experimental investigations of hydraulic fracture growth complexity in slickwater fracturing treatments. San Antonio, Texas. In: SPE137515, presented at the SPE tight gas completions conference; 2010.

[38] Weng X, Kresse O, Cohen C, Wu R, Gu H. Modeling of hydraulic fracture network propagation in a naturally fractured formation. the woodlands, Texas. In: SPE 140253, presented at the SPE hydraulic fracturing technology conference and exhibition; 2011.

[39] Zhang X, Jiang TX, Jia CG, Zhang BP, Zhou J. Physical simulation of hydraulic fracturing of shale gas reservoir. Petrol Drill Tech 2013;41(2):70–4.

[40] Wawersik WR, Stone CM. Character and interpretation of pressure records in anelastic rock with examples of hydraulic fracturing tests in salt. Minneapolis, Minnesota, USA. Proceedings of the 2nd international workshop on Hydraulic fracturing stress measurements. 1988. p. 342–4.

[41] Rummel F, Hansen J. Interpretation of hydrofrac recordings using a simple fracture mechanics simulation model. Int J Rock Mech Min Sci Geomech Abstr 1989;26:483–8.

[42] Cornet FH, Julien P. Stress determination from hydraulic test and focal mechanisms of induced seismicity. Int J Rock Mech Min Sci Geomech Abstr 1989;26:235–8.

[43] Haimson BC. Earthquake related stresses at Rangley. Colorado. Proceedings of 14th US symposium of Rock mechanics. ASCE: University Park; 1973. p. 689–708.

[44] Sengupta S, Subrahmanyam DS, Joseph D, Sinha RK, Kar A. Measurement of in-situ stress by hydrofracture method and investigations on redistribution of in-situ stress due to local tectonics and methods of workings at Tandsi and Thesgora mines. WCL to devise a suitable support plan SSR. Coal S&T Project No. MT-117. 2004. NIRM-GS-99-01.

[45] Guo Tiankui, Zhang Shicheng, Qu Zhanqing, Tong Zhou, Xiao Yongshun, Gao Jun. Experimental study of hydraulic fracturing for shale by stimulated reservoir volume. Fuel 2014;128:373–80. https://doi.org/10.1016/j.fuel.2014.03.029.

[46] Gowd TN, Govardhan M. Stimulation of groundwater borewells by hydraulic fracturing – a simulation study. No. NGRI-87-Environ-32. Report T.R.; 1987.

[47] Damani A, Sharma A, Sondergeld CH, Rai CS. Mapping of hydraulic fractures under triaxial stress conditions in laboratory experiments using acoustic emissions. San Antonio, Texas, USA. In: SPE 159604, presented at the SPE annual technical conference and exhibition; 2012.

[48] Cipolla CL, Warpinski NR, Mayerhofer MJ, Lolon EP, Vincent MC. The relationship between fracture complexity, reservoir properties, and fracture treatment design. Denver, Colorado. In: SPE 115769, presented at the SPE annual technical conference and exhibition; 2010.

[49] Casas LA, Miskimins JL, Black AD, Green SJ. Laboratory hydraulic fracturing test on a rock with artificial discontinuities. San Antonio, Texas, USA. In: SPE 103617, presented at the SPE annual technical conference and exhibition; 2006.

[50] Amadei B, Stephansson O. Rock stress and its measurement. 1st ed. Springer Dordrecht Publisher; 1997XV. https://doi.org/10.1007/978-94-011-5346-1.

[51] Price Jones A, Whittle RA, Hobbs NH. Measurement of *in situ* rock stresses by overcoming. January. Tunnels and tunneling. 1984. p. 12.

[52] Reinecker J, Stephansson O, Zang A. Stress analysis from overcoring data. World stress map project. Guidelines: Overcoring; 2008.

[53] Chen Z, Xue CJ, Jiang TX, Qing YM. Proposals for the application of fracturing by stimulated reservoir volume (SRV) in shale gas wells in China. Nat Gas Ind 2010;30(10): 30–2.

[54] Doe T. Hydraulic fracturing and overcoring stress measurements in a deep borehole at Stripa test mine. Proceedings of 22nd US symposium of rock mechanics. Cambridge (US): MIT Publications; 1981. p. 373–8.

[55] Rummel F. Fracture mechanics approach to hydraulic fracturing stress measurements. Fracture mechanics of rocks. London: Academic Press; 1986. p. 217–39.

[56] Mayerhofer MJ, Lolon EP, Warpinski NR, Cipolla CL, Walser D, Rightmire CM. What is stimulated rock volume (SRV)?. Fort Worth, Texas. In: SPE 119890, presented at the 2008 SPE shale gas production conference; 2008.

[57] Subrahmanyam DS. Evaluation of hydraulic fracturing and overcoring methods to determine and compare the in situ stress parameters in porous rock mass. Geotech Geol Eng 2019;37:4777−87. https://doi.org/10.1007/10706-019-00937-7.
[58] Subrahmanyam DS, Shyam G, Vamshidhar, Shankar K Vikram. Hydraulic fracturing stress measurements in fractured rock mass at a hydroelectric project, India. 7th International Symposium on In-situ Rock Stress. Tampere, Finland; 2016. p. 298−307.
[59] Byerlee JD. The fracture strength and frictional strength of Weber sandstone. Inc. J. Rock Mich. Min. Sci. 1975;12:1−4.
[60] Peshcherenko Aleksandra, Bekerov Ilmir, Chuprakov Dimitry, Abdrazakov Dmitriy. Fast-running model for high-volume hydraulic fracturing. J Petrol Sci Eng 2022;213(110430). https://doi.org/10.1016/j.petrol.2022.110430. ISSN 0920-4105.
[61] Cornet FH. Stress determination from hydraulic tests on preexisting fractures − the HTPF method. In: Proc. Int.Symp.on rock stress and rock stress measurements. Stockholm, Lulea, Sweden: Centek Publ.; 1986. p. 301−12.
[62] Liu JZ, Gao LS, Zhang X. Observations on the acoustic emission in an in-house hydrofracturing simulation experiment. Acta Pet Sin 1990;11(2):73−8.
[63] Subrahmanyam DS, Shyam G, Vamshidhar K, Vikram S. State-of-the-art technique to conduct in situ stress measurements in deep proposed coal-mining blocks of Singareni collieries, India. Curr Sci 2020;119(6):1027−30. https://doi.org/10.18520/cs/v119/i6/1027-1030.
[64] Hubbert MK, Willis DG. Mechanics of hydraulic fracturing. Transactions of Society of Petroleum Engineers of AIME 1957;210:153−63.
[65] Sjoberg J, Christiansson R, Hudson JA. ISRM Suggested methods for rock stress estimation-Part 2: overcoring methods. Int J Rock Mech Min Sci 2003;40:999−1010.
[66] Timoshenko SP, Goodier JN. Theory of elasticity. United Engineering trustees Inc; 1934. p. 567.